Proceedings Paper:

Slay, E. orcid.org/0000-0003-0744-4299, Mancinelli, E., Amer, M. et al. (1 more author) (2024) Modelling and Optimization of Fluid Dynamics, Microparticles and Cell Loading in Microfluidics. In: 2024 46th Annual International Conference of the IEEE Engineering in Medicine and Biology Society (EMBC). 2024 46th Annual International Conference of the IEEE Engineering in Medicine and Biology Society (EMBC), 15-19 Jul 2024, Orlando, FL, USA. Institute of Electrical and Electronics Engineers (IEEE) ISBN 979-8-3503-7150-5

https://doi.org/10.1109/embc53108.2024.10782150

Modelling and Optimization of Fluid Dynamics, Microparticles and Cell Loading in Microfluidics

Ellen Slay
Faculty of Biological Sciences
University of Leeds
Leeds, United Kingdom
bsesl@leeds.ac.uk

Elena Mancinelli
School of School of Electronic and Electrical Engineering
University of Leeds
Leeds, United Kingdom
elem@leeds.ac.uk

Mahetab Amer
Division of Cell Matrix Biology & Regenerative Medicine, School of Biological Sciences,
University of Manchester
Manchester, United Kingdom
mahetab.amer@manchester.ac.uk

Virginia Pensabene
School of School of Electronic and Electrical Engineering.
School of Medicine,
University of Leeds
Leeds, United Kingdom
v.pensabene@leeds.ac.uk

Organ-on-a-chip technology allows for the examination of cell cultures within dynamic systems to better understand biological pathways. The three-dimensional (3D) microenvironment in which cells reside influences their behavior and maturation via mechanobiological cues. Computational fluid dynamics can be used to model the incorporation of biomaterials and 3D constructs as well as in the spreading of cells in microfluidic devices. In our work poly(lactic acid) microparticles (MPs) are used as 3D substrate for mesenchymal stem cells (MSCs) for cancer research within the bone. Computational fluid dynamics (CFDs) was used to predict the behavior of MPs when loaded in microfluidic devices and define the optimal density for cell growth. Predicted efficiency of loading aligned with the observed MPs loaded in the microfluidic devices. A final concentration of 1,160 MPs/µL was then chosen as demonstrated to support the growth of MSCs. This work demonstrates the feasibility of using computational modelling to optimize microfluidic design and particles loading, and to assess the use of biomaterials prior to the undertaking of extensive time-consuming laboratory work in a microfluidic system.

Engineered microenvironments, microfluidics, CFDs, biomaterials, tissue engineering, mesenchymal stem cells.

I. Introduction

The development of microfluidic devices to generate organ-on-a-chip (OOAC) platforms, allows for the culture of cells within a dynamic and complex 3D environment. Such advances have allowed for the development of highly complex models which can be used in biomedical research, drug discovery, as well as pre-clinical testing including those modelling the bone [1-3]. OOACs aim to recapitulate biomechanical cues within tissue micro-environment, such as topography and flow due to their effect on cell behavior and differentiation [4]. Topography is the microscopic surface features that cells interact with and is determined by the hierarchical structure of the ECM and roughness [5]. Interstitial flow is the movement of fluid through the extracellular matrix of tissues [6].

Topography is a dominant cue in determining the behavior of MSCs [7], and has been used to guide their differentiation [8, 9]. Polymeric microparticles (MPs) have been used to drive MSCs down an osteogenic lineage without the use of exogenous osteo-inductive factors [9] and these MPs can be used as a growth surface for cells to model the bone.

Interstitial fluid flow is another important biomechanical cue and has also been shown to influence bone cell behavior and proliferation [10] and to alter levels of bone resorption through affecting osteocytes and paracrine signalling between osteocytes and osteoblasts [11].

Modelling accurate flow when engineering bone models, that incorporate topography, is therefore essential. Computational fluid dynamics (CFDs) constitutes a branch of fluid mechanics employing numerical analysis and data structures to examine dynamics of fluid flow [12]. CFD modelling is applied here for modelling fluid flow in microfluidic devices to ensure physiologically relevant shear stress will be experienced by the cells, and to assess the feasibility of loading and perfusing microfluidic devices with customizable biomaterials.

The purpose of this study is to design a new *in vitro* model of the bone, based on a custom-made microfluidic chamber and polymeric MPs to mimic the natural porous characteristics of the bone. We first completed a finite element model of the medium flow and of the particle aggregation within the microfluidic chamber, then used the results to design the loading and culture protocol and to assess the viability of mesenchymal stem cells (MSCs) in this 3D microenvironment.

II. Methods

A. Flow simulation and the prediction of MP loading

The microfluidic design was created by using computer-aided design software (Autodesk Fusion 360, AutoCAD 2023). The microfluidic device, as shown in Fig. 1, has a total volume of 10.3µL and a surface area of 41mm^2. The design geometry was imported into COMSOL Multiphysics® v6.1. The fluid inside the device was simulated as an incompressible, homogeneous, Newtonian fluid with density (ρ=1000 kg m^{-3}) and viscosity (μ=1×10^{-3} Pa s), with flow rates of 100µL/s to mimic initial loading and 0.5µL/min for long-term culture [13]. A "fine"-mesh 3D COMSOL simulation with a step size of 0.1 s was performed as a finite element model (FEM) with the particle tracing for fluid flow module to compute the motion of particles in a background fluid as a simulation for the loading of MPs.

B. Microfluidic device fabrication and design

Microfluidic devices were fabricated by soft lithography, as previously described [14] and following specification from material datasheets. In brief, a 3" silicon wafer was used as substrate to fabricate the mold in SU8 2075. Polydimethylsiloxane (PDMS; Sigma-Aldrich, USA) was then poured on the mold and cured at 70°C for 4 hours. The PDMS layers were then lifted, and ports were opened using a 1.5mm biopsy puncher to allow loading of fluids. The layers were bonded using oxygen plasma treatment, which allows contamination removal, oxidation and activation of the exposed surfaces. The devices were then filled with sterile water and stored in a petri dish at 4°C until use to preserve hydrophilicity. The devices were sterilized by exposure to UV light for 30 min. Culture media reservoirs (300µL volume) were bonded to the device to support a dynamic perfusion with a syringe pump. Flow is generated within the device with a syringe pump (Harvard) with a constant flow rate of 0.5µl/min and an average recorded outlet flow of 0.4576µl/min over 2 minutes through the use of a 0.4-7µl/min flow rate sensor (Dolomite) (Fig.1).

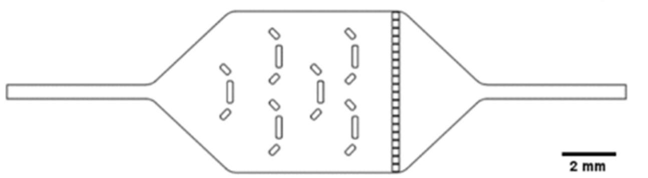

Figure 1. Microfluidic devices. Microfluidic device design, including a chamber (250µm x 5.80mm x 8.60mm) with a 6 trap system (3 blocks each 200 µm wide, one long and 2 short, 692µm and 310µm in length, offset at 136°, spaced at 1.40mm), and pillars 250µm x 250 µm x 250 µm with gaps of 40µm to create a barrier for the microparticles. Scale bar: 2mm.

C. Production of microparticles

Poly(lactic acid) (PLA) microparticles were prepared with PLA (DL09E, Ashland, United Kingdom) by a solvent evaporation oil-in-water emulsion technique, as described previously [9]. The organic phase, containing the PLA in dichloromethane (DCM; ≥99.8, Fisher Scientific, UK) was homogenized (Silverson Homogenizer L5M) for 5 min in 100mL of the aqueous continuous phase, 1% w/v of poly(vinyl acetate-co-alcohol) in deionized (DI) water (PVA; MW 13–23 kDa, 98% hydrolyzed; Sigma-Aldrich, Sweden). The resulting emulsion was stirred continuously at 480 rpm at room temperature to allow for solvent evaporation. To remove residual PVA, MPs were centrifuged and subsequently washed with DI water. Cell strainers with mesh sizes of 40 µm and 70 µm (Corning, USA) were used to separate MPs based on size. The collected MPs were freeze-dried (LyoPro 6000, Heto, UK) for 48 hours and then stored at -20°C. For use in cell culture, the MPs were sterilized with UV light for 30 min and then conditioned with cell culture media for 30 min before media was replaced and cells plated. The number of MPs per mg was calculated using this formula:

$$N = (6x10^{12}/(\pi \cdot \rho S \cdot d^3))/1000 \quad (1)$$

where N= number of microparticles per mg; ρS = density of PLA (1.25 g/cm^3); d = mean diameter (µm).

D. Cell culture and viability assessment

hTERT-immortalized adipose derived Mesenchymal stem cells (MSCs) were obtained from ATCC (ASC52telo) and cultured in Dulbecco's Modified Eagle Medium supplemented with 10% (v/v) fetal bovine serum, 1% (w/v) L-glutamine and 1% (w/v) Penicillin-Streptomycin. Cells were tripsinized, counted and plated at 15,000 cells/cm^2 on the MPs in a cell repellent plate to form aggregates over 24 hours. MPs-MSCs aggregates were then transferred to the devices and tested for viability at 5 days of culture in comparison to 2D cultures at the same seeding density, using ReadyProbes™ (Cell Viability Imaging Kit, Blue/Red, R37610) according to the manufacturer's instructions. Cells were imaged with an EVOS FL Auto 2 fluorescence microscope. All materials were purchased from ThermoFisher.

III. RESULTS

To define the optimal culture conditions (MPs density for cellular adhesion and liquid volume for medium perfusion), we first modelled the microparticles loading into the microfluidic device and then changing the number of particles and over time.

Based on the initial weight of MPs in 100µL of cell culture medium used for loading, we can calculate the effective number of MPs, the total surface area (SA) of the MPs, and the void volume remaining in the system for perfusion (Table 1).

TABLE 1. MPS TO LOADING.

Weight of MPs (mg)	*N* of MPs	SA of MPs seeded [mm^2]	SA of MPs and base [mm^2]	Volume of 1 MP [mm^3]	Volume of MPs [mm^3]	Volume in culture chamber [µl]
0	0	0	41.061	N/A	N/A	10.26525
0.5	5957.942261	47.84998074	88.91098074	6.76787E-05	0.403225806	9.862024194
1	11915.88452	95.69996148	136.7609615	6.76787E-05	0.806451613	9.458798387
2	23831.76904	191.399923	232.460923	6.76787E-05	1.612903226	8.652346774
10	119158.8458	956.9996148	998.0606148	6.76787E-05	8.0645161290	2.200733871

N (number of MPs) = (6e12/(π·ρS·d^3)); ρS = density of PLA (1.25 g/cm^3); d = mean diameter (50 µm). SA (surface area) = (4πr^2). Volume (V) = (4/3 (πr^3)). V of MPs loaded = ((4/3 (πr^3))*N).

To assess the distribution of microparticles within loading varying weights of the MPs within the cell culture chambers, the trajectories of the MPs in the microfluidic devices were simulated in COMSOL and snapshots of the spreading of particles in the chamber were recorded at intervals of 0.1s after loading (Fig. 2).

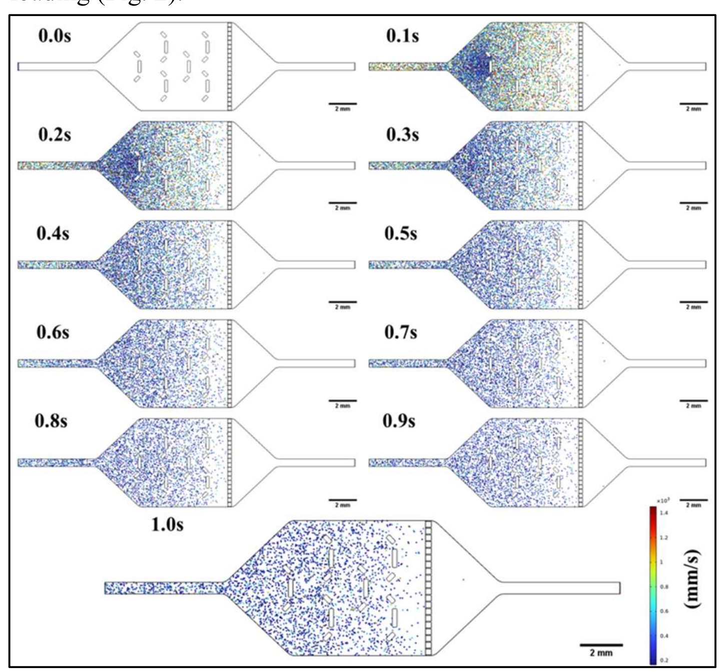

Fig 2. MP trajectories in the microfluidic device. 1mg of MPs were loaded from the inlet channel (left) and dispersion in the chamber was assessed over 1 second at 100µl/second to mimic initial loading. Representative snapshots at intervals of 0.1 s are reported from top to bottom. MP velocity varies from 53.092 to 1476.829 mm/s as shown in the color bar on the bottom right.

This particle trajectory data shows an initial rapid spreading of particles, with MPs velocities ranging 0 to over 1400mm/s in the first milliseconds and the majority of the MPs arresting within 1 second (blue color corresponding to still MPs). We also confirmed that the traps aided the reduction of speed of the microparticles after loading and a homogeneous loading.

The spreading of different weight of microparticles was modelled assuming a flow rate of 0.5µL/minute for 30s. When increasing the initial MPs weight, the chamber was gradually filled, reaching a full coverage with the maximum weight tested (10 mg) (Fig. 3).

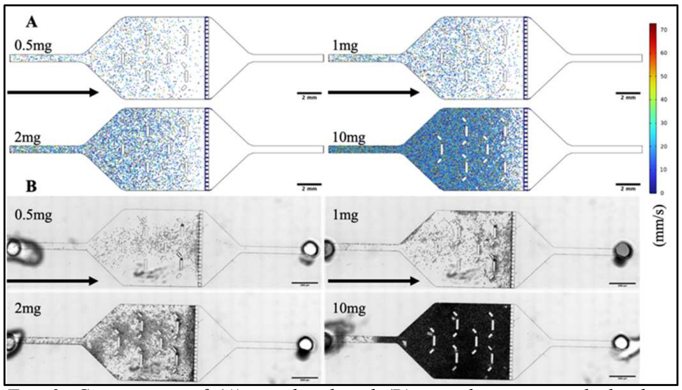

Fig. 3. Comparison of (A) simulated and (B) actual microparticle loading within microfluidic devices. Increasing number and weights of MPs were loaded in suspension directionally from the inlet channel (arrow) and allowed to settle for 30 seconds under gravity generated flow. Scale bar: 2000µm.

When loading 1 mg a homogeneous spreading of the MPs in the chamber was observed, which settled down in the chamber within the first 30 seconds. The higher weights of MPs (2 to 10 mg), the chamber appeared fully covered with very limited void surface remaining, which is a condition we want to exclude. The FEM model provide a quasi-realistic representation of the density and spreading of the MPs in the microfluidic chamber (Fig. 3A). In the experimental sets (Fig. 3B), the MPs move rapidly across the traps and spread heterogeneously, which can be ascribed to structural aspects (e.g. the suboptimal fabrication of the device, possible uneven wettability of the PDMS walls after plasma activation). There is a linear relationship between the number of microparticles loaded compared and the percentage of surface coverage (R^2=0.954 for simulated data and R^2=0.9855 for experimental data).

These results show that the loading of the MPs is directly proportional to the initial MPs weight, and the first parameter to tune the final density of particles in the device. This is helpful to select the best concentration of MPs to use for the next steps of cell loading and OOAC perfusion.

Based on these simulations, calculations, and limited set of loading experiments, 1mg was selected as optimal concentration of MPs for loading, due to the large surface area provided without compromising the perfusion within the device.

Next the microfluidic device was used with the MPs as a growth surface for MSCs to develop a bone model. MSCs showed good viability on the MPs in the microfluidic device 5 days post seeding while cells cultured in the device without MPs, "adherent", showed lower viability, with a high number of dead cells and rounded morphology, which is expected on bare glass and PDMS surfaces, less biocompatible than PLA (Fig. 4).

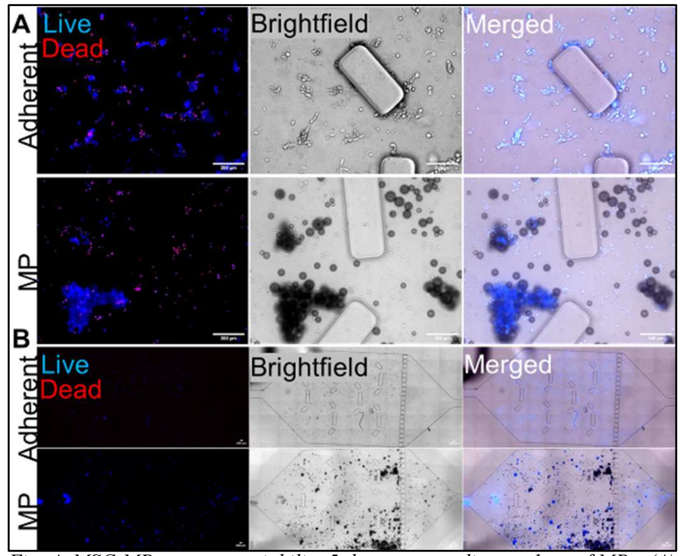

Fig. 4. MSC-MP aggregate viability 5 days post seeding on 1mg of MPs. (A) Single view of a 10x fluorescence image. Scale bar: 200µm. (B) Tiled image of 10x fluorescence image. Scale bar: 1000µm.

IV. DISCUSSION

This study shows the utility of CFDs in the exploration and optimization of biomaterial utilization within microfluidic devices, specifically in elucidating the loading behavior of biomaterials and in sustaining cell cultures.

There are many similarities observed between the CFD simulation of MP loading and the experimental MP behavior, such as the spread of the MPs throughout the device and the distribution of particles per area. There are some notable differences, the first being the final location of the MPs post loading: in experimental settings the MPs reach the micropillars, which serve as a barrier for them, while in the simulation many of the particles do not reach the barrier and arrest within 1 second.

In the simulation the MPs at the barrier remain at a thickness of 1 MP deep and do not aggregate to the same extent as is observed in the experiments. The simulation utilizes the particle tracking module which does not take into consideration the particle-particle interactions, it allows for multiple particles to occupy the same space, observed in the density seen in Fig. 3.A. at the barrier, however the simulation, therefore cannot account for a buildup of MPs from the barrier into the culture chamber as is seen in the experiments (Fig. 3.B.).

Additionally, in the real conditions, MPs cluster behind the traps, suggesting there is backflow of the MPs within the chamber where they have bounced off other barriers and they cluster in areas where the flow is reduced. This phenomenon is not taken in account in the simulations due to the laminar flow assumptions used which excludes backflow, but the velocity profile does show regions of reduced flow behind the traps (data not shown).

Another difference between the experimental and simulated results is that of the behavior of the MPs at the wall of the microfluidic device. In the experimental setting the MPs interact with the device wall in an undefined manner, this is particularly clear in the loading of 1mg of MPs in Fig. 3, whereas in the simulations the MPs interact through diffuse scattering when they encounter the device walls. Through exploring the PDMS-PLA interaction it is shown that both polymers are hydrophobic with water contact angles of the PDMS at 108±7°[15] and of the dimpled microparticles at 90±3° [9], thus suggesting no electrostatic interactions and the use of diffuse scattering in the simulation is applicable.

Future simulations could incorporate multiple flow rates within a single simulation however this is beyond the current capabilities of this simulation, thus the two simulations were studied in tandem. Another potential improvement within the simulation involves refining the model by utilizing a finer mesh; a fine mesh was used with an average quality of 0.6812, where 0.0 represents a degenerated element and 1.0 represents the best possible element. Whilst it is understood that by using a finer mesh within COMSOL this will increase the accuracy of the model [16], considering the computational efficiency and the risk that the solver might not converge at an extreme, the scale finer was used for simulations [17].

By confirming the trajectory and velocity of the MPs we can confidently transition from the simulated setup to the laboratory, and the application of a 1mg MP concentration, ensures a sufficient fraction of the chamber volume (9.459 µl) for the culture media, thereby providing crucial support for sustained cell viability. Despite the notable presence of dead cells on the uncoated PDMS, the device does exhibit the ability to maintain viable cells for a duration of 5 days. This observation confirms the biocompatibility of PDMS and MPs, however the increased dead cells within the Adherent group does suggest that the MPs are a better cell growth surface than the PDMS, this is further supported by the proportion of dead cells on the PDMS around the viable cells present on the MPs.

Further development of this model would include varying flow rates to best support the differentiation of MSCs and the inclusion of multiple cell types to generate a dynamic bone system. Previous research has shown that a similar flow rate affects MSC function and protein production [18].

The simulation results confirmed the functionality of CFD for modelling complex OOAC platforms, for pre-assessment of fluid dynamics before device fabrication and extensive laboratory work. In this way, these findings highlight the robustness of the microfluidic system for cell culture studies and demonstrates avenues for further simulation refinement and experimental exploration in the development of a physiologically relevant bone OOAC.

V. Acknowledgment

The authors would like to thank Prof. Christoph Walti and Dr. Benjamin Johnson at the University of Leeds for providing access, technical guidance and feedback on the microfabrication and the CFD methods.

References

[1] J. Scheinpflug, M. Pfeiffenberger, A. Damerau, F. Schwarz, M. Textor, A. Lang, et al. Journey into Bone Models: A Review. Genes, 2018. 9(5): p. 247.

[2] H. Bahmaee, R. Owen, L. Boyle, C. M. Perrault, A. A. Garcia-Granada, G. C. Reilly, et al., Design and Evaluation of an Osteogenesis-on-a-Chip Microfluidic Device Incorporating 3D Cell Culture. Front Bioeng Biotechnol, 2020. 8: p. 557111.

[3] S. Hao, L. Ha, G. Cheng, Y. Wan, Y. Xia, D. M. Sosnoski, et al., A Spontaneous 3D Bone-On-a-Chip for Bone Metastasis Study of Breast Cancer Cells. Small, 2018. 14(12): p. 1702787.

[4] E. E. Slay, F. C. Meldrum, V. Pensabene and M. H. Amer., Embracing Mechanobiology in Next Generation Organ-On-A-Chip Models of Bone Metastasis. Front Med Technol, 2021. 3: p. 722501.

[5] F. M. Watt and W. T. S. Huck, Role of the extracellular matrix in regulating stem cell fate. Nature Reviews Molecular Cell Biology, 2013. 14(8): p. 467-473.

[6] W. Yao, Y. Li, and G. Ding, Interstitial Fluid Flow: The Mechanical Environment of Cells and Foundation of Meridians. Evidence-Based Complementary and Alternative Medicine, 2012. 2012: p. 1-9.

[7] A.J. Engler, H.L. Sweeney, and D.E. Discher, Matrix elasticity directs stem cell lineage specification. Cell, 2006: p. 677-89.

[8] A. Prasopthum, M. Cooper, K. M. Shakesheff and J. Yang, Three-Dimensional Printed Scaffolds with Controlled Micro-/Nanoporous Surface Topography Direct Chondrogenic and Osteogenic Differentiation of Mesenchymal Stem Cells. ACS Appl Mater Interfaces, 2019. 11(21): p. 18896-18906.

[9] M. H. Amer, M. Alvarez-Paino, J. McLaren, F. Pappalardo, S. Trujillo, J. Q. Wong, et al., Designing topographically textured microparticles for induction and modulation of osteogenesis in mesenchymal stem cell engineering. Biomaterials, 2021. 266: p. 120450.

[10] D. Sheyn, D. Cohn-Yakubovich, S. Ben-David, S. De Mel, V. Chan, C. Hinojosa, et al., Bone-chip system to monitor osteogenic differentiation using optical imaging. Microfluid Nanofluidics, 2019. 23(8).

[11] C. Wittkowske, G. C. Reilly, D. Lacroix and C. M. Perrault Bone Cell Models: Impact of Fluid Shear Stress on Bone Formation. Front Bioeng Biotechnol, 2016. 4: p. 87.

[12] J. Blazek, Computational Fluid Dynamics: Principles and Applications. 3rd ed. 2015: Butterworth-Heinemann.

[13] J.X.J. Zhang and K. Hoshino, Chapter 3 - Microfluidics and Micro Total Analytical Systems, Molecular Sensors and Nanodevices. 2014: William Andrew Publishing.

[14] Y. Xia and G.M. Whitesides, Soft Lithography. Angewandte Chemie International Edition, 1998. 37(5): p. 550-575.

[15] M. H. Wu, J. P. G. Urban, Z. Cui and Z. F. Cui, Development of PDMS microbioreactor with well-defined and homogenous culture environment for chondrocyte 3-D culture. Biomedical Microdevices, 2006. 8(4): p. 331-340.

[16] R.W. Pryor, Multiphysics Modeling Using COMSOL: A First Principles Approach. 1st ed. 2009, Sudbury, MAUnited States: Jones and Bartlett Publishers, Inc. 872.

[17] X. Xu, Z. Li, and A. Nehorai, Finite element simulations of hydrodynamic trapping in microfluidic particle-trap array systems. Biomicrofluidics, 2013. 7(5): p. 054108.

[18] W. Yi, Y. Sun, X. Wei, C. Gu, X. Dong, X. Kang, et al. Proteomic profiling of human bone marrow mesenchymal stem cells under shear stress. Molecular and Cellular Biochemistry, 2010. 341(1-2): p. 9-16.